Characterization and Application of Nanomaterials (2023) Volume 6 Issue 2
doi: 10.24294/can.v6i2.3182

ORIGINAL RESEARCH ARTICLE

An eco-friendly route for green synthesis of ZnO-$CoFe_2O_4$ nanoparticles from cardamom and ginger extract as an efficient electrochemical catalyst for water oxidation

Aynaz Kamyab[1], Mir Hadi Banan Khojasteh[1], Karim Asadpour-Zeynali[1,2,*]

[1] *Department of Analytical Chemistry, Faculty of Chemistry, University of Tabriz, Tabriz 51666-16471, Iran*

[2] *Pharmaceutical Analysis Research Center, Faculty of Pharmacy, Tabriz University of Medical Sciences, Tabriz 51664-14766, Iran*

*** Corresponding author:** Karim Asadpour-Zeynali, asadpour@tabrizu.ac.ir

ABSTRACT

Water splitting has been one of the potential techniques as a clean and renewable energy resource for the fulfillment of world energy demands. One of the major aspects of this procedure is the exploitation of efficient and inexpensive electrocatalysts due to the fact that the water oxidation procedure is accompanied by a delayed reaction. In this research, ZnO-$CoFe_2O_4$ nanostructure was successfully synthesized via the green method and green resources from cardamom seeds and ginger peels for oxygen evolution reaction (OER). The modified Glassy carbon electrode (GCE) with ZnO-$CoFe_2O_4$ is effective for the electrochemical water oxidation interaction since it has sufficient electrical strength and excellent catalytic performance. The creation of rice-like and small granular structures of ZnO-$CoFe_2O_4$ nano-catalysts was confirmed by characterization methods such as XRD, FESEM, EDS and MAP. According to the achieved results, in the electrolysis of water, with in-cell voltage of 1.40 V and 50 mA cm^{-2} for current density in a 0.1 M KOH electrolyte and OER only has 170 mV overpotentials.

Keywords: green synthesis; nanoparticles; ZnO-$CoFe_2O_4$; cardamoms; ginger peels

ARTICLE INFO

Received: 16 October 2023
Accepted: 24 November 2023
Available online: 4 December 2023

1. Introduction

In today's world fossil fuels are exploited as the primary resource of energy to meet world demands which in turn has led to the energy crisis, great harm to the environment, global warming and other issues[1,2]. Thus, the development and application of an eco-friendly and renewable energy resource to decrease the usage of conventional fossil fuel is crucial for a sustainable economy and community[3]. In this regard, hydrogen (H_2), as a suitable mass-energy density and non-carbonous emission source, exhibits an efficient capability for sustainable energy production which can be replaced with fossil fuel[4,5]. Electrochemical water splitting is an effective method to achieve hydrogen with high purity at the cathode and this electrochemical process includes two half reactions, known as an oxygen evolution reaction (OER) and a hydrogen evolution reaction (HER) at the anode at the cathode, respectively[6,7]. In real-world experiments, electrochemical reduction of water involves an excessive overpotential[8] which means, introducing sufficient modifiers to activate proton reduction by the lowest possible overvoltage for the HER reaction and enhance the kinetics of OER is an indispensable stage for the current demands[9,10]. The most efficient water splitting

performance to date has been developed by means of noble metal-based electrocatalysts, principally Pt-based and Ir/Ru-based electrocatalysts for HER and OER procedures, respectively[11,12]. Nonetheless, the precious metals' expensiveness and their scarceness are major reasons for water splitting limitations on an industrial scale. Thus, the investigation of non-precious options with sufficient activity and stability is imperative[13–15].

Spinel ferrites-based compounds as cobalt ferrite nanostructures have various utilities in information storage and electronic devices[16,17], drug delivery[18], biological[19], and environmental[20] owing to the essential properties like inexpensiveness, mechanical hardness, excellent stability, acceptable curie temperature and high magnetic anisotropy. Moreover, cobalt ferrite has a small band gap, which results in an increment in decomposition performance[21,22]. Recently, ZnO semiconductors with exclusive properties like a nonpoisonous nature, band gap of roughly 3.3 eV, remarkable photosensitivity and thermal stabilities[23]. Photocatalytic activity results due to the movement of photogenerated holes and electrons to the surface which conduce pollutant degradation under UV and visible irradiations[24,25]. Surface modifying, doping and coupling with other compounds like semiconductors are instances of the approaches that are employed to improve the catalytic performance of ZnO[26–28]. Cerium oxide is an excellent example of this agenda that is utilized in diverse research like gas sensors, H_2S removal, eco-friendly pigments, catalyst and etc.[29–33].

Several procedures have been established to produce ZnO-$CoFe_2O_4$, including, hydrolysis of chelated zinc diethylene glycol alkoxide complexes in alkaline diethylene glycol solution at high temperature[34] and hydrothermal method with carbon nanoparticles as the template[24], microwave combustion[35], co-precipitation[36], sol-gel procedure accompanied by hydrothermal technique[37], and combustion process[38,39]. Nevertheless, the aforementioned techniques involve sophisticated processes, intricate equipment, consuming chemicals, and high energy consumption, thus contributing to undesirable impacts on the ecosystem. Biogenic resources are drawing growing attention because of their sustainability. Some biogenic ingredients are recyclable and have possibility to be achieved from waste compounds, which substantially decreases their production expenditure[40–43]. More significantly, biogenic resources have the possibility to be manipulated to include definite catalytic features, making them an effectual choice for selective procedures[44,45]. These resources not only provide eco-friendly substitutes to synthetic catalysts due to biodegradability and non-toxicity, but also show enhanced stability and activity which make them adequate for various applications such as water splitting[46–48]. A promising approach for green synthesis is a hydrothermal method due to the fact that it employs water as a solvent and natural plants leaf extracts such as Solanum nigrum[49], Aloe vera[50] Azadirachta indica[51], and Camellia sinensis[52] as capping agents which monitor the nanoparticles of the chosen elements. One more example of a natural component been exploited for this agenda to produce NiO nanocrystals is rambutan (*Nephelium lappaceum* L.) peel extract from Sapindaceae spices[53].

In this paper, ZnO-$CoFe_2O_4$ semiconductor magnetic nanoparticles were produced by consuming cardamom and ginger peel extract. The benefits of this procedure involve the use of inexpensive, harmless and environmentally friendly materials, and an uncomplicated and time-saving process. The main element in cardamom and ginger peel extract is phenolic combinations acting as a capping agent, stabilizer and even chelating agent in order to capture the metal ions and monitor the formation of nanostructures. The morphology and structure of the synthesized ZnO-$CoFe_2O_4$ were investigated with XRD, FESEM, EDS and MAP techniques. In addition, the electrochemical interactions ZnO-$CoFe_2O_4$ in the OER process were assessed by monitoring cyclic voltammetry (CV), linear sweep voltammograms (LSV) and chronoamperometry techniques for stability analysis and Tafel calculation in basic conditions.

2. Experimental

2.1. Reagents

Zinc acetate dihydrate ($[Zn(CH_3CO_2)_2]\cdot 2H_2O$) and sodium hydroxide (NaOH) were bought commercially

from Sigma-Aldrich Chemicals. Compounds which are employed during this research were analytical grade and did not treat with any purification approaches also, deionized water was utilized in all experiments of this research. Fresh cardamom seeds and ginger peels were bought from a local health store. All glassware were completely cleaned before executing each test and protective procedures was taken to prevent any contamination. The Potassium hydroxide (KOH), Iron Nitrate ($Fe(NO_3)_3 \cdot 9H_2O$), Hydrogen chloride (HCl 37%) solution, Cobalt Nitrate ($Co(NO_3)_2 \cdot 6H_2O$), and Ethanol were provided from MERCK.

2.2. Synthesizing and preparation methods

2.2.1. Green synthesis of ZnO

Fresh cardamoms were washed with distilled water to eliminate all contaminations, and then fully dried. The standard protocol accompanying little modification was employed to prepare the extract. First 5 g of cardamoms were boiled in 100 mL distilled water for 20 min at 80 °C, and the extract was obtained from filter paper at room temperature. The resulting filtered extract was utilized for further investigation. In order to prepare 0.2 M zinc acetate solution 2.2 g of powdered ($[Zn(CH_3CO_{2)2}] \cdot 2H_2O$) was poured in 50 mL of distilled H_2O and stirred on a magnetic stirrer until fully dissolution. Then, 50 mL of this extract was added gradually to 50 mL of $[Zn(CH_3CO_2)_2] \cdot 2H_2O$ accompanying continuous solution stirring, which was followed by drop-by-drop addition of 10 mL of 1 M NaOH solution. A yellowish-white sediment was attained instantly after pouring sodium hydroxide solution. In the next step, the precipitate was washed with ethanol three times and centrifugated at 5000 rpm for 10 min and the precipitate was separated and completely dried in a vacuum. Finally, ZnO-NPs green sedimentation was calcinated at 400 ℃ in a muffle furnace.

2.2.2. $CoFe_2O_4$ green synthesis

20 g of ginger root were sliced into 100 mL of deionized water and the admixture underwent a boiling process for 5 min, the color of the solution altered to yellow (pH ~ 6). Then temperature of this extract decreased at room temperature and filtered. Also, 10 g of cardamom seeds were ground and resulted in yellow-brown sediment was added and stirred in 100 mL of deionized water after 4 h of boiling, the precipitate was separated from the solution and the brown separated sediment was cooled at room temperature. In the next step, metal nitrates ($2Fe^{3+}$:$1Co^{2+}$) were added gradually within stirring conditions to the aqueous seeds extract, respectively. Then these combinations (pH ~ 2) were brought to a gel-like concentration with a thermal treatment process at 80 ℃ and these gels were heated at 250–300 ℃ which is accompanied by an initial gel melting process which is followed by a spontaneous self-ignition, leaving behind a magnetic foam (self-combustion). During this exothermic procedure, the admixture of nitrates and plant extracts acts in the same way as common oxidants and fuels. The final step was the calcination of the magnetic foams at 800 ℃ for 1 h in order to enhance the crystallization degree.

2.3. Characterization of catalysts and electrochemical performance

The crystalline structure was investigated with the X-ray diffraction analysis with SIEMENS D500 and 2θ spectra range from 10 to 80. In order to investigate the morphology of the synthesized nanostructure FESEM (model: TESCAN and MIRA3). Also, the chemical structure of the developed nanostructures was further investigated with an EDS attached to FESEM and FT-IR analysis was executed with Shimadzu 8400 (Japan).

Electrochemical analyses were executed by mean of an EG&G Model 273 Potentiostat/Galvanostat instrument accompanied with GCE as a working electrode, an Ag/AgCl electrode as a reference electrode and a platinum as a counter electrode (there electrode system), all these electrodes were bought from Azar Electrode Co., Urmia, Iran. During the study, the standard reversible hydrogen electrode (RHE) was utilized to calculate the electrochemical potentials. The Nernst Equation (1):

$$E_{RHE} = E_{Ag/AgCl} + 0.059\ pH\ (13) + E^0_{Ag/AgCl} \quad (1)$$

which was employed to convert the obtained potential based on the Ag/AgCl to the RHE potential (Equation

2).

$$E_{Ag/AgCl} = 0.198 \text{ V (at 25 Celsius degree temperature)} \quad (2)$$

Also, the 0.1 M KOH is used as electrolyte. In order to accomplish OER analysis, linear sweep voltammetry (LSV) and CV assessment were performed at a scan rate of and potential limit of 0–1.6 V vs. Ag/AgCl. Furthermore, its stability in the basic solution was studied by the chronoamperometry technique. The Tafel slope is achieved from Equation (3):

$$\eta = b \times log\left(\frac{j}{j_0}\right) \quad (3)$$

(η: overpotential, b: Tafel slope, j: current density, j_0: exchange current density[54,55]).

3. Result and discussion

3.1. Characterization

3.1.1. X-ray diffraction investigation

Synthesized ZnO-$CoFe_2O_4$ NPs exhibited sharp diffraction peaks which is a testimony to the decent crystallinity of this synthesis illustrated in **Figure 1**. Diverse peaks relating to the 2θ value were obtained in 31.9, 34.5, 36.2, 40.6, 42.7 56.6, 62.9, 66.4, 68 and 69.36. Moreover, the characteristic peaks relating to (hkl) values of (111), (220), (311), (222), (400), (511), and (440). These values are in accordance with the hexagonal Wurtzite structure of ZnO based on the Joint Committee on Powder Diffraction Studies Standards. The X-ray diffraction results of the nanostructure attained from the self-combustion procedure utilizing the aqueous extract of ginger and cardamom accepted the correct synthesis of Zn-$CoFe_2O_4$ which is in good agreement previously reported research. The purity of produced nanoparticles was confirmed by the absence of any other peak[56,57].

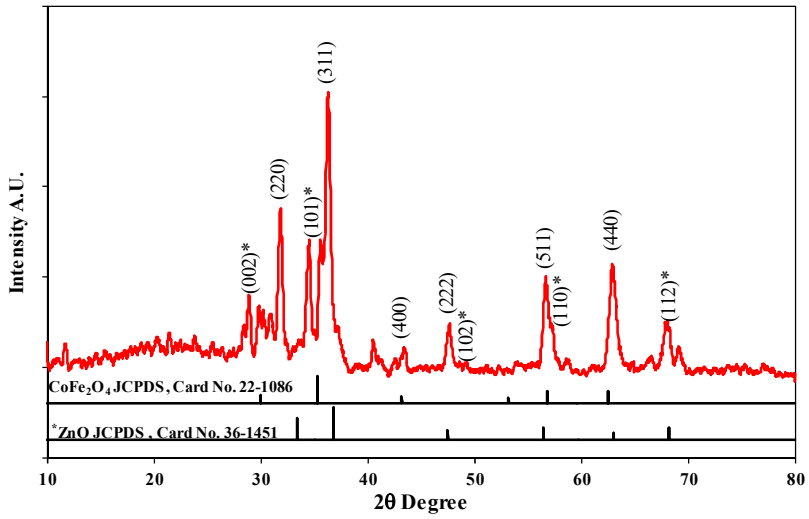

Figure 1. XRD pattern of green synthesized ZnO-$CoFe_2O_4$.

3.1.2. FESEM & EDX

In order to investigate the green synthesized ZnO-$CoFe_2O_4$ NPs morphological characteristics field emission scanning electron microscopy (FESEM) was exploited. FESEM micrographs of the nanostructure in 200 nm (**Figure 2**) demonstrated the synthesizing of very fine nanograined agglomerates with equiaxed nanocrystals. SEM analysis of the nanoparticles in 500 nm (**Figure 3**) confirms the existence of porous nanograined agglomerates structure with the mainstream remaining equiaxed and limited faceted crystals. Based on the micrograph image, a rod-shaped and identic ordination is observable which is in good accordance

with green approaches for producing ZnO-$CoFe_2O_4$ NPs. As its observable EDX spectroscopy results in the samples attained utilizing ginger and cardamom green extract, all the expected major elements including Co, O, Fe and Zn were detected. XRD and EDS graphs are an indication of successful synthesis for a three-component nanostructure[58,59].

3.1.3. FTIR analysis

In order to investigate the possible interaction between ZnO and $CoFe_2O_4$ and sustain the formation of ZnO-$CoFe_2O_4$ spinel structure, the FTIR spectra of ginger root and cardamom seeds aqueous extracts were accomplished from 400 to 4000 cm^{-1} and the obtained spectra exhibited major bands of phenolic hydroxyl group (-OH) representing hydrogen bonding in flavonoids (**Figure 4**). The interaction of ZnO and $CoFe_2O_4$ causes an alteration in the Zn-O and Fe-O bond absorption area. Furthermore, emerging two significant bands between 400–800 cm^{-1} wavelength were assigned to the stretching vibration of the Fe-O bond and the stretching vibration of Zn-O and Co-O in the three composite structures[60]. The peaks at 556 and 454 cm^{-1} are attributed to the stretching vibration of the Fe-O and Co-O bond. The peaks at around 546 cm^{-1} are attributed to the stretching vibration of the Fe-O bond and the peaks around 410–432 cm^{-1} to the stretching vibration of Zn-O and Co-O in the composite samples.

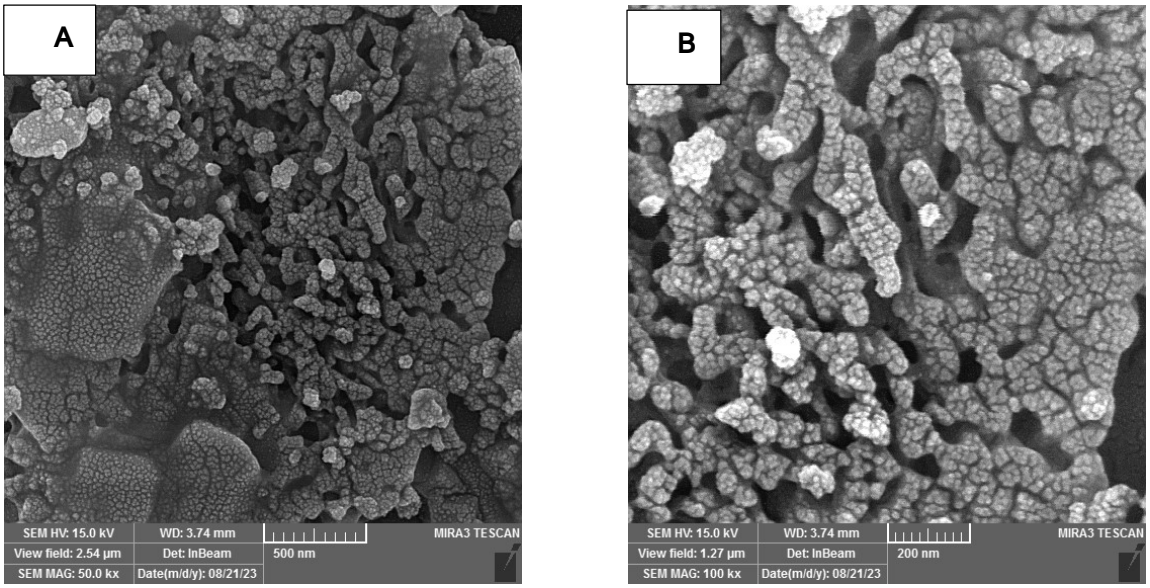

Figure 2. SEM image of ZnO-$CoFe_2O_4$ nanostructure in **(A)** 500 nm and **(B)** 200 nm scales.

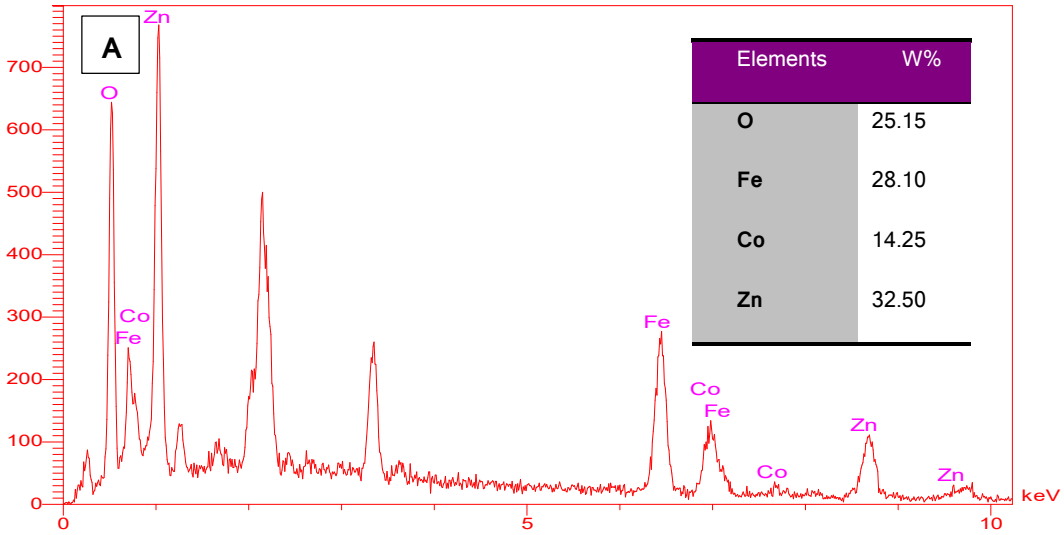

Figure 3. (*Continued*).

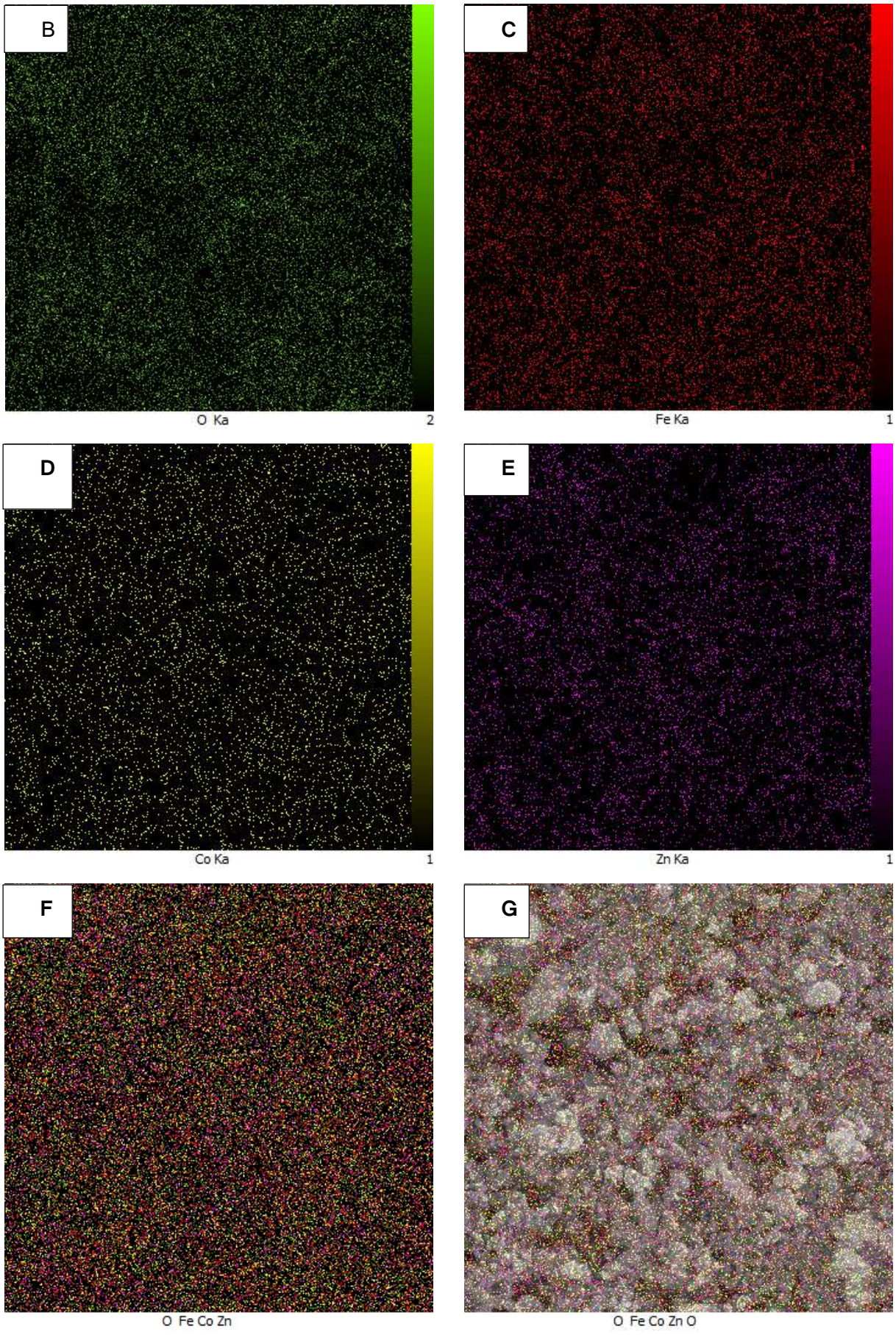

Figure 3. **(A)** EDS and mapping images of ZnO-$CoFe_2O_4$ nanostructures, **(B)**–**(E)** its elements mapping separately, **(F)** the elements mapping simultaneously and **(G)** mapping and SEM simultaneously.

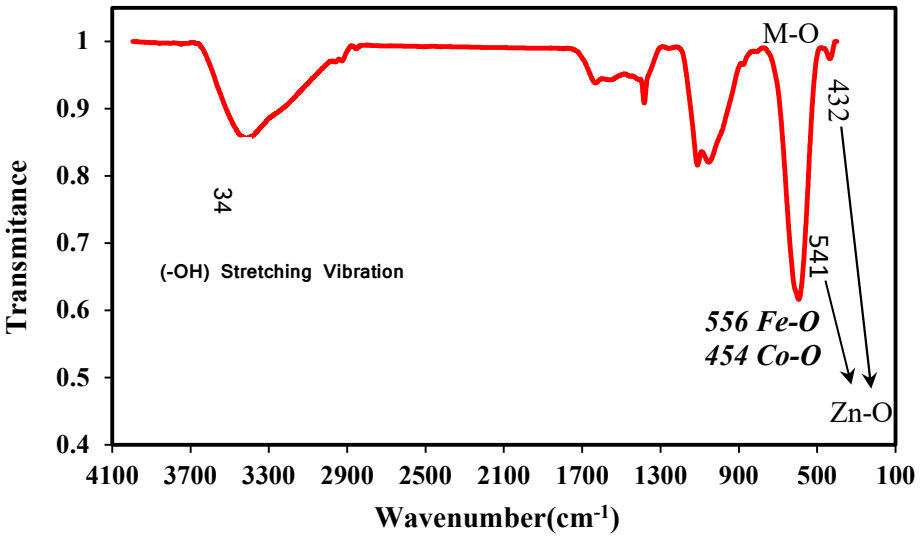

Figure 4. FTIR spectra of ZnO-$CoFe_2O_4$ nanoparticles.

3.1.4. UV–Vis spectroscopy analysis

UV–Vis diffuse reflectance analysis was performed to explore the optical properties of the ZnO-$CoFe_2O_4$ nanostructure. ZnO absorbs well in the UV region and it has little stimulation in the visible light wavelength, however, $CoFe_2O_4$ indicates appropriate absorption in the visible region. As it is observable from **Figure 5**, the characteristic peak of green ZnO-$CoFe_2O_4$ was detected around 350 nm which resulted due to a high value of excitation binding energy. This result is in a good agreement with previous research which approves the correct synthesizing of ZnO-$CoFe_2O_4$ NPs[61].

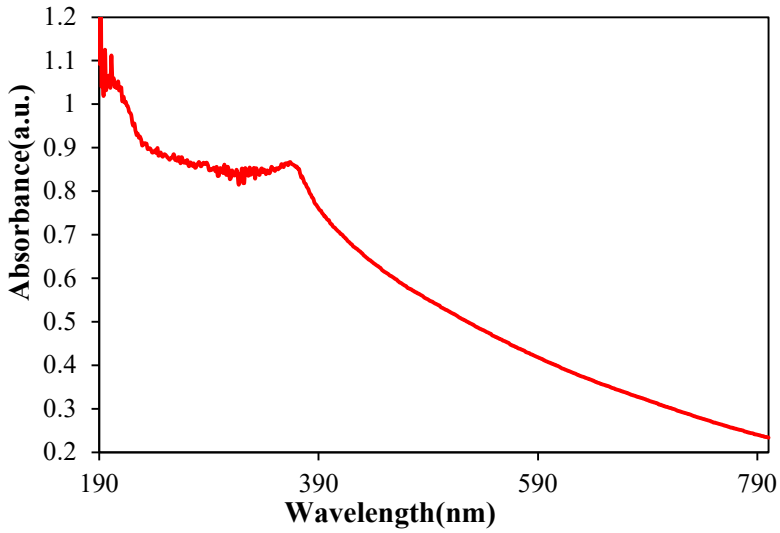

Figure 5. UV-Visible spectra ZnO-$CoFe_2O_4$ nanocomposite.

3.2. Electrochemical measurements

In this research, a conventional three electrode system within 1 M Potassium hydroxide and 0.6–2.5 V vs. HRE voltage range and a scan rate of 10 mV S^{-1} was employed. As is observable in **Figure 6**, the LSV plots of bare GCE and ZnO-$CoFe_2O_4$ modified GCE were studied in the aforementioned situation. Polarization plots evaluation demonstrates the minimum electrocatalytic activity of bare GCE, while ZnO-$CoFe_2O_4$/GCE shows satisfactory catalytic performance for OER with 170 mV for overpotential at 50 mA cm^{-2}, diminishing overpotential defines enhancement in the kinetics of the OER process. What's more, ZnO-$CoFe_2O_4$/GCE as

noble-metal-free electrocatalysts in basic situations is desperately active for OER, which can be assigned to the synergistic impact of the ZnO and the $CoFe_2O_4$ nanoparticles. In addition, the attendance of ZnO in the ZnO-$CoFe_2O_4$/GCE heterostructure improves the electrocatalyst electrical conductivity to increase the electrocatalytic performance. Moreover, ZnO and $CoFe_2O_4$ nanostructures create a 3D ZnO-$CoFe_2O_4$ nanostructure with more existing active sites, providing more ways for the operative electrons transfer, and conductive GCE offers a platform for growing active materials, which helps electrical conductivity between the GCE and the developed electrocatalysts. According to obtained LSV plots, the oxygen evolution peak of ZnO-$CoFe_2O_4$/GCE is located at ~1.42 V vs. RHE.

Tafel plot was utilized for the OER catalytic kinetics evaluation. As it is illustrated in **Figure 7**, the ZnO-$CoFe_2O_4$/GCE has the lowest Tafel slope with 88.56 mV dec^{-1}. Also, the ZnO and $CoFe_2O_4$ exhibit higher Tafel slop of 121.1 and 167.57, respectively, which means ZnO-$CoFe_2O_4$/GCE displays a faster kinetic and enhanced catalytic performance for OER.

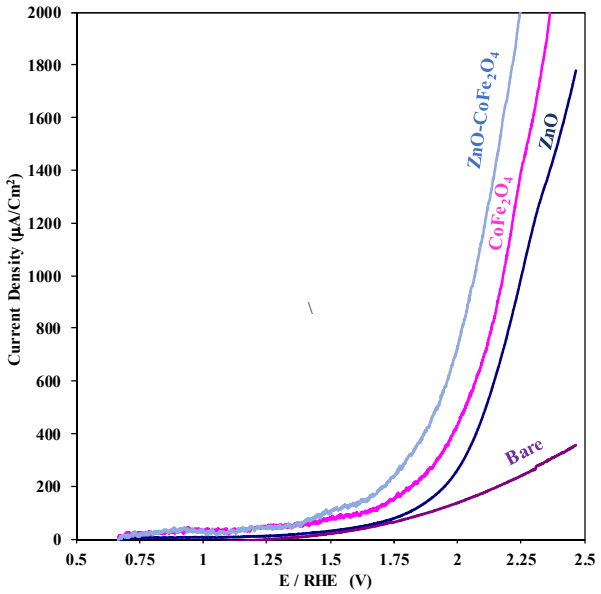

Figure 6. Linear sweep voltammograms of ZnO-$CoFe_2O_4$, $CoFe_2O_4$, ZnO and bare electrode.

Considering the lower overpotential and Tafel slope, which can be a good proof for the respective activity of ZnO-$CoFe_2O_4$/GCE synthesized by adequate hydrothermal approach, ZnO-$CoFe_2O_4$/GCE was selected as an ideal electrocatalyst in this present investigation. Based on the lower Tafel slope value and overpotential of the ZnO-$CoFe_2O_4$/GCE catalyst is an illustration for faster performance and sufficient kinetics toward OER activity than other synthesized catalysts.

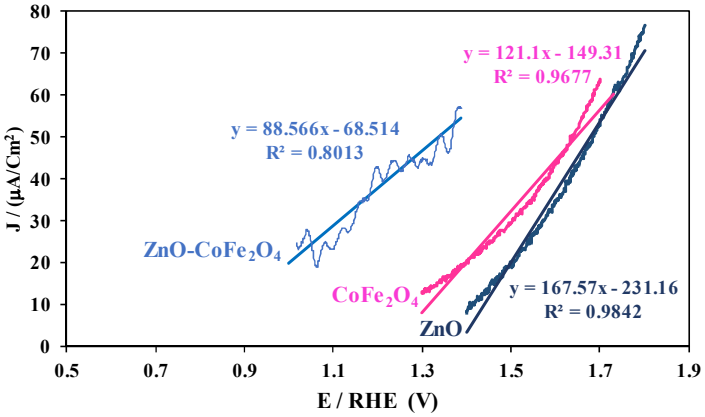

Figure 7. Tafel plots of Zn-$CoFe_2O_4$, $CoFe_2O_4$ and ZnO nano catalysts.

One of the major criterions for every catalyst in electrochemistry is its electrochemical stability which can be analyzed with the chronoamperometry method. Undoubtedly, the current density and time (j-t) plot indicated the premiere electrochemical stability of ZnO-$CoFe_2O_4$/GCE for a 15 h electrolysis reaction under a basic situation (**Figure 8**). Instantaneously, the catalytic stability of ZnO-$ZnFe_2O_4$/GCE before and after 500 cycles was examined by continuous sweeps and, the polarization plot of ZnO-$CoFe_2O_4$/GCE after 500 cycles exhibited insignificant variation from that initial condition.

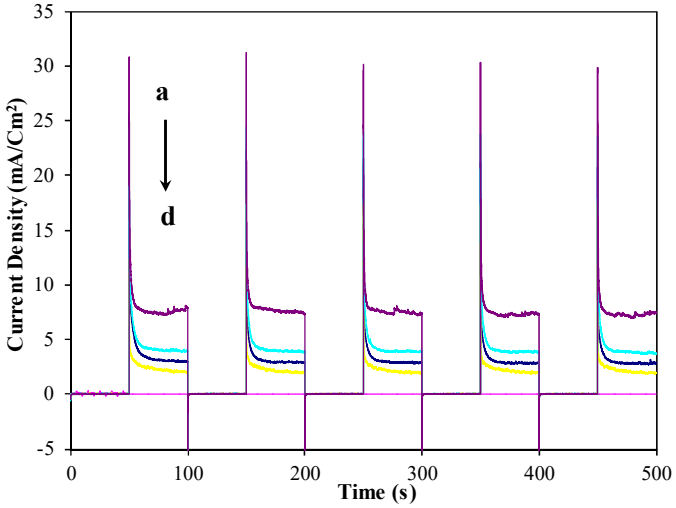

Figure 8. Chronoamperometry plots of ZnO-$CoFe_2O_4$ modified electrode with potential steps of (a) 0–1.2, (b) 0–1.1, (c) 0–0.10 and (d) 0–0.9 V in 0.1 M KOH solution.

In order to compare the efficiency of the catalysis prepared by the green method with other catalysts that have been published for water oxidation in recent years, **Table 1** has been prepared. As can be seen in this table, the Tafel slope and overpotential of this research are comparable to the results in the literature.

Table 1. Comparison of the OER activities of some recently reported catalysts for water oxidation.

Catalyst	Tafel slope (mV dec^{-1})	Solution	Over potential (mV)	Current density	References
Aloe-vera-mediated NiOx	95	NaOH	413	10 mA cm^{-2}	[62]
MoO_4^{2-} intercalating α-$Co(OH)_2$ nanosheet	57.78	1 M KOH	303	10 mA cm^{-2}	[63]
Ni–FeOOH/$Ni(OH)_2$	16.8	1 M KOH	264	20 mA cm^{-2}	[64]
$Pr_3Ir_{1-x}Mo_xO_7$	50.52	0.1 M $HClO_4$	259	10 mA cm^{-2}	[65]
Zn-doped RuO_2	41.2	0.5 M H_2SO_4	173	10 mA cm^{-2}	[66]
Ni-Fe-Co film	34.7	1 M KOH	314	10 mA cm^{-2}	[67]
CoMn-LDH@CuO/Cu_2O	89	1 M KOH	297	10 mA cm^{-2}	[68]
$CaFe_6Ge_6$/NF	43.35	1 M KOH	322	10 mA cm^{-2}	[69]
SF[Fe-Tol-Ni]	103	1 M KOH	480	1 mA cm^{-2}	[70]
Ni-FeOOH/NF	52	1 M KOH	277	100 mA cm^{-2}	[71]
Co_3O_4/Pr_2O_3	78	Alkaline	257	10 mA cm^{-2}	[72]
Co_3O_4@$KNbO_3$	61	1 M KOH	330	10 mA·cm^{-2}	[73]
ZnO-$CoFe_2O_4$	88.56	0.1 M KOH	170	50 μA cm^{-2}	This work

4. Conclusion

A green and facile procedure for synthesizing the innovative, effective and stable ZnO-$CoFe_2O_4$ electrocatalyst as a modifier for GCE was introduced, which exhibits a noteworthy OER performance in alkaline circumstances. Additionally, ZnO-$CoFe_2O_4$/GCE has an acceptable specific surface area and porous structure and enhanced accessible active sites and the rate of electron transfer that provides the OER exceptional performance accompanying a low overpotential of 222 mV and a Tafel slope of 88.56 mV dec^{-1} for OER. The kinetics of water oxidation were studied with the Tafel slope technique. Demanding a voltage of 1.45 V at 5 mA cm^{-2} in a water oxidation procedure within three electrode system is a demonstration of

excellent electrochemical efficiency for the ZnO-$CoFe_2O_4$/GCE This work developed a mixed transition metal as an inexpensive electrocatalyst for stable and green OER analysis in basic situations, which has the capability to be employed in other applications like renewable energy storage and other energy conversion methods. This research also provides a novel strategy for accomplishing effective water oxidation with nanostructured transition metals. We assign this outstanding water oxidation activity to the excellent synergistic effects, in situ evolution on the stable conductive substrate and attendance of active OER compounds.

Author contributions

Conceptualization, KAZ and MHBK; methodology, AK and MHBK; software, MHBK; validation, AK and MHBK; formal analysis, MHBK; investigation, AK and MHBK; resources, KAZ; data curation, AK and MHBK; writing—original draft preparation, AK and MHBK; writing—review and editing, KAZ; visualization, AK and MHBK; supervision, KAZ; project administration, KAZ; funding acquisition, KAZ. All authors have read and agreed to the published version of the manuscript.

Acknowledgements

The financial support from the University of Tabriz is gratefully acknowledged.

Conflict of interest

The authors report that there is no conflict of interest to declare.

References

1. Kalair A, Abas N, Saleem MS, et al. Role of energy storage systems in energy transition from fossil fuels to renewables. *Energy Storage* 2021; 3(1): e135. doi: 10.1002/est2.135
2. Anwar MN, Fayyaz A, Sohail NF, et al. CO_2 utilization: Turning greenhouse gas into fuels and valuable products. *Journal of Environmental Management* 2020; 260: 110059. doi: 10.1016/j.jenvman.2019.110059
3. Mehravaran M, Aber S, Asadpour-Zeynali K. Combining the bioelectricity generation with Photo-Electrocatalytic reduction of CO_2 for pollutants degradation and ethanol generation. *Journal of Electroanalytical Chemistry* 2023; 941: 117541. doi: 10.1016/j.jelechem.2023.117541
4. Yapicioglu A, Dincer I. Performance assesment of hydrogen and ammonia combustion with various fuels for power generators. *International Journal of Hydrogen Energy* 2018; 43(45): 21037–21048. doi: 10.1016/j.ijhydene.2018.08.198
5. Yadav GD. In pursuit of the net zero goal and sustainability: Hydrogen economy, carbon dioxide refineries, and valorization of biomass & waste plastic. *AsiaChem Magazine* 2023; 3(1): 110–123. doi: 10.51167/acm00046
6. Shahparast S, Asadpour-Zeynali K. α-MnO_2/FeCo-LDH on nickel foam as an efficient electrocatalyst for water oxidation. *ACS OMEGA* 2023; 8(1): 1702–1709. doi: 10.1021/acsomega.2c07580
7. van der Zalm JM, Quintal J, Hira SA, et al. Recent trends in electrochemical catalyst design for hydrogen evolution, oxygen evolution, and overall water splitting. *Electrochimica Acta* 2023; 439: 141715. doi: 10.1016/j.electacta.2022.141715
8. Sun H, Xu X, Kim H, et al. Electrochemical water splitting: Bridging the gaps between fundamental research and industrial applications. *Energy & Environmental Materials* 2022; 6(5): e12441. doi: 10.1002/eem2.12441
9. Eftekhari A. Tuning the electrocatalysts for oxygen evolution reaction. *Materials Today Energy* 2017; 5: 37–57. doi: 10.1016/j.mtener.2017.05.002
10. Nong HN, Oh H-S, Reier T, et al. Oxide-supported $IrNiO_x$ core–shell particles as efficient, cost-effective, and stable catalysts for electrochemical water splitting. *Angewandte Chemie* 2015; 54(10): 2975–2979. doi: 10.1002/anie.201411072
11. Li Y, Sun Y, Qin Y, et al. Recent advances on water-splitting electrocatalysis mediated by noble-metal-based nanostructured materials. *Advanced Energy Materials* 2020; 10(11): 1903120. doi: 10.1002/aenm.201903120
12. Jo W-K, Moru S, Tonda S. Cobalt-coordinated sulfur-doped graphitic carbon nitride on reduced graphene oxide: An efficient metal–(N,S)–C-class bifunctional electrocatalyst for overall water splitting in alkaline media. *ACS Sustainable Chemistry & Engineering* 2019; 7(18): 15373–15384. doi: 10.1021/acssuschemeng.9b02705
13. Yu Y, Wang T, Zhang Y, et al. Recent progress of transition metal compounds as electrocatalysts for electrocatalytic water splitting. *The Chemical Record* 2023; 23(11): e202300109. doi: 10.1002/tcr.202300109
14. Shih AJ, Monteiro MCO, Dattila F, et al. Water electrolysis. *Nature Reviews Methods Primers* 2022; 2: 84. doi: 10.1038/s43586-022-00164-0

15. Yang H, Huang Y, Teoh WY, et al. Molybdenum selenide nanosheets surrounding nickel selenides sub-microislands on nickel foam as high-performance bifunctional electrocatalysts for water splitting. *Electrochimica Acta* 2020; 349: 136336. doi: 10.1016/j.electacta.2020.136336
16. Rethinasabapathy M, Ezhil Vilian AT, Hwang SK, et al. Cobalt ferrite microspheres as a biocompatible anode for higher power generation in microbial fuel cells. *Journal of Power Sources* 2021; 483: 229170. doi: 10.1016/j.jpowsour.2020.229170
17. Qian H-S, Hu Y, Li Z-Q, et al. ZnO/$ZnFe_2O_4$ magnetic fluorescent bifunctional hollow nanospheres: Synthesis, characterization, and their optical/magnetic properties. *The Journal of Physical Chemistry C* 2010; 114(41): 17455–17459. doi: 10.1021/jp105583b
18. Kiani A, Davar F, Bazarganipour M. Influence of verjuice extract on the morphology, phase, and magnetic properties of green synthesized $CoFe_2O_4$ nanoparticle: Its application as an anticancer drug delivery. *Ceramics International* 2022; 48(23): 34895–34906. doi: 10.1016/j.ceramint.2022.08.079
19. Abdel Maksoud MIA, El-Sayyad GS, Ashour AH, et al. Synthesis and characterization of metals-substituted cobalt ferrite [$M_xCo_{(1-x)}$ Fe_2O_4; (M = Zn, Cu and Mn; x = 0 and 0.5)] nanoparticles as antimicrobial agents and sensors for Anagrelide determination in biological samples. *Materials Science and Engineering: C* 2018; 92: 644–656. doi: 10.1016/j.msec.2018.07.007
20. Mariosi FR, Venturini J, da Cas Viegas A, Bergmann CP. Lanthanum-doped spinel cobalt ferrite ($CoFe_2O_4$) nanoparticles for environmental applications. *Ceramics International* 2020; 46(3): 2772–2779. doi: 10.1016/j.ceramint.2019.09.266
21. Londoño-Calderón CL, Londoño-Calderón A, Menchaca-Nal S, et al. Magnetic properties of cobalt ferrite octahedrons obtained from calcination of granular nanotubes growing on bacterial nanocellulose. *Journal of Magnetism and Magnetic Materials* 2020; 495: 165899. doi: 10.1016/j.jmmm.2019.165899
22. Sudarsan S, Anandkumar M, Trofimov EA. Synthesis and characterization of copper ferrite nanocomposite from discarded printed circuit boards as an effective photocatalyst for Congo red dye degradation. *Journal of Industrial and Engineering Chemistry* 2023; In press. doi: 10.1016/j.jiec.2023.10.020
23. Raizada P, Sudhaik A, Singh P. Photocatalytic water decontamination using graphene and ZnO coupled photocatalysts: A review. *Materials Science for Energy Technologies* 2019; 2(3): 509–525. doi: 10.1016/j.mset.2019.04.007
24. Wilson A, Mishra SR, Gupta R, Ghosh K. Preparation and photocatalytic properties of hybrid core–shell reusable $CoFe_2O_4$–ZnO nanospheres. *Journal of Magnetism and Magnetic Materials* 2012; 324(17): 2597–2601. doi: 10.1016/j.jmmm.2012.02.009
25. Shekofteh-Gohari M, Habibi-Yangjeh A, Abitorabi M, Rouhi A. Magnetically separable nanocomposites based on ZnO and their applications in photocatalytic processes: A review. *Critical Reviews in Environmental Science and Technology* 2018; 48(10–12): 806–857. doi: 10.1080/10643389.2018.1487227
26. Dhiman P, Rana G, Kumar A, et al. ZnO-based heterostructures as photocatalysts for hydrogen generation and depollution: A review. *Environmental Chemistry Letters* 2022; 20: 1047–1081. doi: 10.1007/s10311-021-01361-1
27. Ong CB, Ng LY, Mohammad AW. A review of ZnO nanoparticles as solar photocatalysts: Synthesis, mechanisms and applications. *Renewable and Sustainable Energy Reviews* 2018; 81: 536–551. doi: 10.1016/j.rser.2017.08.020
28. Labhane PK, Sonawane SH, Sonawane GH, et al. Influence of Mg doping on ZnO nanoparticles decorated on graphene oxide (GO) crumpled paper like sheet and its high photo catalytic performance under sunlight. *Journal of Physics and Chemistry of Solids* 2018; 114: 71–82. doi: 10.1016/j.jpcs.2017.11.017
29. Saranya J, Sreeja BS, Padmalaya G, et al. Microwave thermally assisted porous structured cerium oxide/zinc oxide design: Fabrication, electrochemical activity towards Pb Ions, anticancer assessment in HeLa and VERO cell lines. *Journal of Inorganic and Organometallic Polymers and Materials* 2021; 31: 1279–1292. doi: 10.1007/s10904-020-01809-x
30. Ar Rahim D, Fang W, Wibowo H, et al. Review of high temperature H_2S removal from syngas: Perspectives on downstream process integration. *Chemical Engineering and Processing–Process Intensification* 2023; 183: 109258. doi: 10.1016/j.cep.2022.109258
31. Bansal R, Nair S, Pandey KK. UV resistant wood coating based on zinc oxide and cerium oxide dispersed linseed oil nano-emulsion. *Materials Today Communications* 2022; 30: 103177. doi: 10.1016/j.mtcomm.2022.103177
32. Mirzai M, Akhlaghian F, Rahmani F. Photodegradation of ciprofloxacin in water using photocatalyst of zinc oxide nanowires doped with copper and cerium oxides. *Water and Environment Journal* 2020; 34(3): 420–431. doi: 10.1111/wej.12477
33. Shanmugam N, Thirumal V, Kannadasan N, et al. Influence of cerium and nickel Co-doping on ZnO nanostructures for electrochemical behavior of H_2O_2 sensing applications. *Sustainability* 2022; 14(10): 6353. doi: 10.3390/su14106353
34. Zheng J, Song X, Liu X, et al. Synthesis of hexagonal $CoFe_2O_4$/ZnO nanoparticles and their electromagnetic properties. *Materials Letters* 2012; 73: 143–146. doi: 10.1016/j.matlet.2012.01.035
35. Dippong T, Levei EA, Cadar O. Recent advances in synthesis and applications of MFe_2O_4 (M = Co, Cu, Mn, Ni, Zn) nanoparticles. *Nanomaterials* 2021; 11(6): 1560. doi: 10.3390/nano11061560
36. Yadav D, Shukla R. Structural, morphological, optical, magnetic and photocatalytic properties of ZnO/$CoFe_2O_4$

nanocomposites. *Kinetics and Catalysis* 2023; 64: 603–615. doi: 10.1134/S0023158423050129
37. Sathishkumar P, Pugazhenthiran N, Mangalaraja RV, et al. ZnO supported $CoFe_2O_4$ nanophotocatalysts for the mineralization of Direct Blue 71 in aqueous environments. *Journal of Hazardous Materials* 2013; 252–253: 171–179. doi: 10.1016/j.jhazmat.2013.02.030
38. Rahmayeni, Devi A, Stiadi Y, et al. Preparation, characterization of ZnO/$CoFe_2O_4$ magnetic nanocomposites and activity evaluation under solar light irradiation. *Journal of Chemical and Pharmaceutical Research* 2015; 7(95): 139–146.
39. Castro TJ, da Silva SW, Nakagomi F, et al. Structural and magnetic properties of ZnO–$CoFe_2O_4$ nanocomposites. *Journal of Magnetism and Magnetic Materials* 2015; 389: 27–33. doi: 10.1016/j.jmmm.2015.04.036
40. Madhukara Naik M, Bhojya Naik HS, Nagaraju G, et al. Green synthesis of zinc doped cobalt ferrite nanoparticles: Structural, optical, photocatalytic and antibacterial studies. *Nano-Structures & Nano-Objects* 2019; 19: 100322. doi: 10.1016/j.nanoso.2019.100322
41. Chitralekha, Thakur OP, Gaurav S, et al. Green synthesis of ZnO-$CoFe_2O_4$ nanocomposite and study of its structural and electrical behavior along with hydroelectric cell application. In: Sethuraman B, Jain P, Gupta M (editors). *Recent Advances in Mechanical Engineering*, Proceedings of the 1st International Conference on Sustainable Technologies and Advances in Automation, Aerospace and Robotics; 16–17 December 2022; Bhopal (Online), Madhya Pradesh, India. Springer; 2023. pp. 543–553. doi: 10.1007/978-981-99-2349-6_49
42. Tatarchuk T, Shyichuk A, Sojka Z, et al. Green synthesis, structure, cations distribution and bonding characteristics of superparamagnetic cobalt-zinc ferrites nanoparticles for Pb(II) adsorption and magnetic hyperthermia applications. *Journal of Molecular Liquids* 2021; 328: 115375. doi: 10.1016/j.molliq.2021.115375
43. Mosleh-Shirazi S, Kasaee SR, Dehghani F, et al. Investigation through the anticancer properties of green synthesized spinel ferrite nanoparticles in present and absent of laser photothermal effect. *Ceramics International* 2023; 49(7): 11293–11301. doi: 10.1016/j.ceramint.2022.11.329
44. Bardhan SK, Gupta S, Gorman ME, Ali Haider M. Biorenewable chemicals: Feedstocks, technologies and the conflict with food production. *Renewable and Sustainable Energy Reviews* 2015; 51: 506–520. doi: 10.1016/j.rser.2015.06.013
45. Guterl J-K, Sieber V. Biosynthesis “debugged”: Novel bioproduction strategies. *Engineering in Life Sciences* 2013; 13: 4–18. doi: 10.1002/ELSC.201100231
46. Dershwitz P, Bandow NL, Yang J, et al. Oxygen generation via water splitting by a novel biogenic metal ion-binding compound. *Applied and Environmental Microbiology* 2021; 87(14): e0028621. doi: 10.1128/AEM.00286-21
47. Raut SD, Shinde NM, Nakate YT, et al. Coconut-water-mediated carbonaceous electrode: A promising eco-friendly material for bifunctional water splitting application. *ACS OMEGA* 2021; 6(19): 12623–12630. doi: 10.1021/acsomega.1c00641
48. Bachheti RK, Fikadu A, Bachheti A, Husen A. Biogenic fabrication of nanomaterials from flower-based chemical compounds, characterization and their various applications: A review. *Saudi Journal of Biological Sciences* 2020; 27(10): 2551–2562. doi: 10.1016/j.sjbs.2020.05.012
49. Ramesh M, Anbuvannan M, Viruthagiri G. Green synthesis of ZnO nanoparticles using *Solanum nigrum* leaf extract and their antibacterial activity. *Spectrochimica Acta Part A: Molecular and Biomolecular Spectroscopy* 2015; 136: 864–870. doi: 10.1016/j.saa.2014.09.105
50. Manikandan A, Sridhar R, Arul Antony S, Ramakrishna S. A simple aloe vera plant-extracted microwave and conventional combustion synthesis: Morphological, optical, magnetic and catalytic properties of $CoFe_2O_4$ nanostructures. *Journal of Molecular Structure* 2014; 1076: 188–200. doi: 10.1016/j.molstruc.2014.07.054
51. Bhuyan T, Mishra K, Khanuja M, et al. Biosynthesis of zinc oxide nanoparticles from *Azadirachta indica* for antibacterial and photocatalytic applications. *Materials Science in Semiconductor Processing* 2015; 32: 55–61. doi: 10.1016/j.mssp.2014.12.053
52. Senthilkumar S, Sivakumar T. Green tea (Camellia sinensis) mediated synthesis of zinc oxide (ZnO) nanoparticles and studies on their antimicrobial activities. *International Journal of Pharmacy and Pharmaceutical Science* 2014; 6(6): 461–465.
53. Yuvakkumar R, Suresh J, Joseph Nathanael A, et al. Rambutan (*Nephelium lappaceum* L.) peel extract assisted biomimetic synthesis of nickel oxide nanocrystals. *Materials Letters* 2014; 128: 170–174. doi: 10.1016/j.matlet.2014.04.112
54. Sakita AMP, Vallés E, Della Noce R, Benedetti AV. Novel NiFe/NiFe-LDH composites as competitive catalysts for clean energy purposes. *Applied Surface Science* 2018; 447: 107–116. doi: 10.1016/j.apsusc.2018.03.235
55. Yang JW. *Nanostructured Heterojunction Photoelectrodes for Unassisted Photoelectrochemical Water Splitting* [PhD thesis]. Seoul National University; 2023. 208p.
56. Kiani MN, Butt MS, Gul IH, et al. Synthesis and characterization of cobalt-doped ferrites for biomedical applications. *ACS OMEGA* 2023; 8(4): 3755–3761. doi: 10.1021/acsomega.2c05226
57. Oo KM, Aung ZZM, Thant SS. Synthesis and characterization of cobalt zinc ferrite nanoparticles. *Technological University Lashio Journal of Research & Innovation* 2020; 1(2): 132–134.
58. Rahmayeni, Azizah N, Stiadi Y, et al. Magnetic particles nanorod of ZnO/$CuFe_2O_4$ prepared by green synthesized

approach: Structural, optical and magnetic properties, and photocatalytic activity. *Materials Research* 2022; 25: e20210164. doi: 10.1590/1980-5373-MR-2021-0164
59. Naghizadeh M, Taher MA, Tamaddon AM. Facile synthesis and characterization of magnetic nanocomposite $ZnO/CoFe_2O_4$ hetero-structure for rapid photocatalytic degradation of imidacloprid. *Heliyon* 2019; 5(11): e02870. doi: 10.1016/j.heliyon.2019.e02870
60. Mansournia M, Ghaderi L. Single- and double-shelled $CoFe_2O_4$ nanoparticles as highly efficient magnetic separable photocatalysts. *ChemistrySelect* 2019; 4(1): 24–30. doi: 10.1002/slct.201803496
61. Rahmayeni, Alfina A, Stiadi Y, et al. Green synthesis and characterization of $ZnO\text{-}CoFe_2O_4$ semiconductor photocatalysts prepared using rambutan (*Nephelium lappaceum* L.) peel extract. *Materials Research* 2019; 22(5): e20190228. doi: 10.1590/1980-5373-MR-2019-0228
62. Selvanathan V, Shahinuzzaman M, Selvanathan S, et al. Phytochemical-assisted green synthesis of nickel oxide nanoparticles for application as electrocatalysts in oxygen evolution reaction. *Catalysts* 2021; 11(12): 1523. doi: 10.3390/catal11121523
63. Meng Y-L, Li Y, Tan Z, et al. Hierarchical MoO_4^{2-} intercalating $\alpha\text{-}Co(OH)_2$ nanosheet assemblies: Green synthesis and ultrafast reconstruction for boosting electrochemical oxygen evolution. *Energy & Fuels* 2021; 35(3): 2775–2784. doi: 10.1021/acs.energyfuels.0c03836
64. Hao X, Chen F, Zhang Y, et al. Magnetic-field-assisted electrodeposition regulates the Ni:Fe ratio for water oxidation. *Materials Today Sustainability* 2023; 24: 100556. doi: 10.1016/j.mtsust.2023.100556
65. Chen S, Zhang S, Guo L, et al. Reconstructed Ir–O–Mo species with strong Brønsted acidity for acidic water oxidation. *Nature Communications* 2023; 14: 4127. doi: 10.1038/s41467-023-39822-6
66. Zhang D, Li M, Yong X, et al. Construction of Zn-doped RuO_2 nanowires for efficient and stable water oxidation in acidic media. *Nature Communications* 2023; 14: 2517. doi: 10.1038/s41467-023-38213-1
67. Xu Y, Lin Q, Sun Y, et al. Electrochemical/photoelectrochemical water splitting on self-limiting electrodeposited iron-group mutual alloys. *Journal of The Electrochemical Society* 2023; 170: 056511. doi: 10.1149/1945-7111/acd663
68. Hameed A, Zulfiqar F, Iqbal W, et al. Electrocatalytic water oxidation on $CuO\text{–}Cu_2O$ modulated cobalt-manganese layered double hydroxide. *RSC Advances* 2022; 12(45): 28954–28960. doi: 10.1039/D2RA05036F
69. Yang H, Niklas Hausmann J, Hlukhyy V, et al. An intermetallic $CaFe_6Ge_6$ approach to unprecedented Ca−Fe−O electrocatalyst for efficient alkaline oxygen evolution reaction. ChemCatChem 2022; 14(14): e202200293. doi: 10.1002/cctc.202200293
70. Cao Y, Su Y, Xu L, et al. Oxygen vacancy-rich amorphous FeNi hydroxide nanoclusters as an efficient electrocatalyst for water oxidation. *Journal of Energy Chemistry* 2022; 71: 167–173. doi: 10.1016/j.jechem.2022.03.044
71. Li L, Wang Z, She X, et al. Ni-modified FeOOH integrated electrode by self-source corrosion of nickel foam for high-efficiency electrochemical water oxidation. *Journal of Colloid and Interface Science* 2023; 652: 789–797. doi: 10.1016/j.jcis.2023.08.112
72. Saleem MK, Jabbour K, Niaz NA, et al. Facile engineering of Co_3O_4/Pr_2O_3 nanostructure for boosted oxygen evolution reaction. *Applied Physics A* 2023; 129: 833. doi: 10.1007/s00339-023-07101-2
73. Zhang J, Chen J, Chen Y, et al. The synergistic effect of Co_3O_4 and $KNbO_3$ in $Co_3O_4@KNbO_3$ composite for enhanced performance of water oxidation. *Materials Letters* 2023; 352: 135178. doi: 10.1016/j.matlet.2023.135178